11th World Congress on Computational Mechanics (WCCM XI)
5th European Conference on Computational Mechanics (ECCM V)
6th European Conference on Computational Fluid Dynamics (ECFD VI)
E. Oñate, J. Oliver and A. Huerta (Eds)

THERMAL CONDUCTION IN FGM AND MLC SHELL STRUCTURES

STEPHAN KUGLER*, PETER A. FOTIU* AND JUSTIN MURIN†

* Department of Applied and Numerical Mechanics,
University of Applied Sciences Wiener Neustadt, Wiener Neustadt, Austria,
kugler@fhwn.ac.at, fotiu@fhwn.ac.at and http://www.fhwn.at

† Department of Applied Mechanics and Mechatronics,
FEI, Slovak University of Technology in Bratislava, Slovakia,
justin.murin@stuba.sk and http://www.stuba.sk

Key words: Thermal Conduction, Shell Structures, Transverse Temperature Field

Abstract. Precise thermo-elastic analyses of structures made of functionally graded materials (FGM) or multi-layer composites (MLC) require accurate temperature distributions with respect to the membrane direction and with respect to the thickness direction. Here, a novel algorithm is proposed which evaluates those fields properly in case of convection boundary conditions applied onto the top and bottom surface, respectively. Numerical results indicate efficiency and accuracy of the proposed approach.

1 Introduction

This paper focuses on the analysis of thermal effects in shell structures of thickness h made of functionally graded materials (FGM) or multilayer composites (MLC). The constitutive model is characterized by a variation of material properties over the volume under consideration to achieve specific functions and applications. This variation is continuous in FGMs and discontinuous in MLCs. Here, we concentrate only on arbitrary variations of material properties in transverse direction. Variations with respect to the membrane directions can be modeled easily using a discretization scheme with elements each showing constant variations with respect to the elemental membrane plane. FGM and MLC structures play an important role in sensors and actuators (see [1] and references therein) and accurate virtual analysis procedures are required.

Here, we propose a novel algorithm to accurately evaluate temperature fields $T(\hat{x}, \hat{y}, \hat{z})$ in structures which show arbitrary continuous or discontinuous variations of thermal conductivity $k(\hat{z})$ with respect to the transverse direction $\hat{z}$. The geometrical mid-surface of the structure is discretized with quadrilateral elements. A thermal boundary value problem is solved with respect to two kinds of boundary conditions:

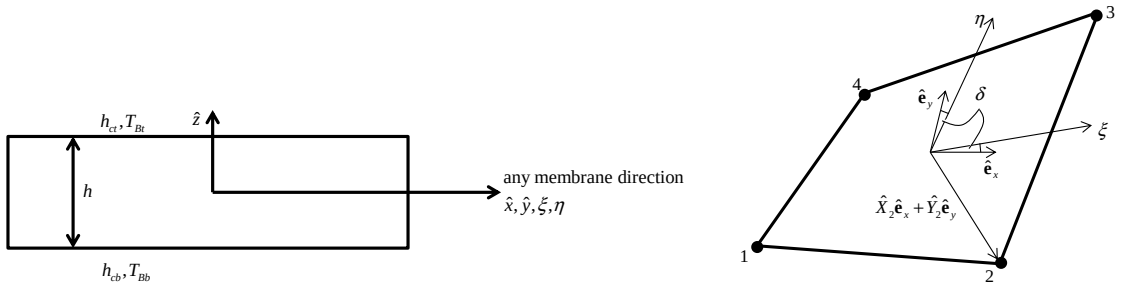

(a) Description of the thermal field problem (b) Elemental coordinate system

Figure 1: Discretized problem

- A Dirichlet-type boundary condition: The mean temperature $\overline{T}$ can be prescribed at any node.
- A von Neumann-type boundary condition: Convection can be applied independently onto the top- and bottom-surface and the non-constant temperature distribution with respect to the thickness direction has a prescribed gradient there.

The present paper is organized as follows: In Sect. 2 the numerical framework to evaluate the temperature field $T(\hat{x}, \hat{y}, \hat{z})$ is discussed. There, it is a main issue to decompose the temperature distribution into a mean temperature

$$\overline{T}(\hat{x}, \hat{y}) = \frac{1}{h} \int_h T(\hat{x}, \hat{y}, \hat{z}) d\hat{z} \tag{1}$$

discussed in Sect. 2.1, and into a transverse distribution $\theta_1(\hat{z})$ or $\theta_2(\hat{z})$ proposed in Sect. 2.2. Then, the temperature field reads

$$T(\hat{x}, \hat{y}, \hat{z}) = \overline{T}(\hat{x}, \hat{y}) + \theta_1(\hat{z}) = \overline{T}(\hat{x}, \hat{y})\theta_2(\hat{z}). \tag{2}$$

In Sect. 3 one numerical example is given in order to show the good predictive quality of the proposed approach, and in Sect. 4 conclusions are drawn.

2 Numerical framework

In this section an approach is given to evaluate the temperature field $T(\hat{x}, \hat{y}, \hat{z})$ within the shell's volume. The problem is characterized by a FGM or MLC shell structure of thickness h with a transversely varying thermal conductivity k, where convection is applied onto the outer surfaces. Fig. 1a shows a cut through the shell structure, and we see that convection is applied independently onto the top- and bottom-surface, i.e.

$$\hat{z} = -h/2: \quad q_n^b = h_{cb}(T(\hat{z} = -h/2) - T_{Bb}), \tag{3}$$

$$\hat{z} = h/2: \quad q_n^t = h_{ct}(T(\hat{z} = h/2) - T_{Bt}). \tag{4}$$

Here, $\hat{x}$ and $\hat{y}$ refer to an elemental Cartesian coordinate system (Fig. 1b), while ξ and η denote parameter coordinates ($-1 \leq \xi \leq 1$ and $-1 \leq \eta \leq 1$). Correspondingly, $\hat{z}$ describes the thickness direction of the discretized shell structure. Without loss of generality, we use four noded quadrilateral shell elements in this paper. In (3) and (4) h_{ct} and h_{cb} denote the convection coefficient on the top and bottom surface, while T_{Bt} and T_{Bb} refers to the corresponding fluid temperatures.

As introduced in (2) the solution can be decomposed into the analysis of the mean temperature field $\overline{T}(\hat{x}, \hat{y})$ and into the transverse temperature field $\theta_1(\hat{z})$ or $\theta_2(\hat{z})$,

$$\theta_2(\hat{z}) = 1 + \frac{\theta_1(\hat{z})}{\overline{T}}. \tag{5}$$

The solution strategy is iterative while each iteration consists of two steps:

1. Evaluation of the mean temperature $\overline{T}(\hat{x}, \hat{y}) = {}^1\!/\!_h \int_h T(\hat{x}, \hat{y}, \hat{z})\, d\hat{z}$ in membrane direction

2. Estimate the temperature distribution in transverse direction $\theta_1(\hat{z})$ and $\theta_2(\hat{z})$ based on a mean temperature $\overline{T}$.

An iterative procedure with iteration number I is required since the shell's surface temperatures are not known within the first step. Thus, (3) and (4) cannot be satisfied exactly. We resolve that problem by rewriting (3) and (4) according to

$$\begin{aligned} \hat{z} = -{}^h\!/\!_2: \quad & q_n^{b\,I+1} = h_{cb}(\overline{T}^{I+1} - T_{Bb}^{*I}), \\ \hat{z} = {}^h\!/\!_2: \quad & q_n^{t\,I+1} = h_{ct}(\overline{T}^{I+1} - T_{Bt}^{*I}), \end{aligned} \tag{6}$$

with

$$\begin{aligned} T_{Bb}^{*I} &= T_{Bb} - \theta_1^I(\hat{z} = -{}^h\!/\!_2), \\ T_{Bt}^{*I} &= T_{Bt} - \theta_1^I(\hat{z} = {}^h\!/\!_2). \end{aligned} \tag{7}$$

The global iterative algorithm can be summarized as follows:

Algorithm 1 Global iterative algorithm

1. $I = 0$
2. $\theta_1^{I=0}(\hat{z} = \pm h/2) = 0$
3. WHILE tolerance not reached ($e <$ tol - given tolerance)
   (a) $T_{Bb}^{*I} = T_{Bb} - \theta_1^I(\hat{z} = -h/2)$ and $T_{Bt}^{*I} = T_{Bt} - \theta_1^I(\hat{z} = h/2)$
   (b) FIND $\overline{T}^{I+1}$ according to Sect. 2.1 using convection boundary condition (6) and (6).
   (c) FIND θ_1^{I+1} according to Sect. 2.2
   (d) $I = I + 1$

The formulation of the tolerance is problem dependent, however, for most applications it should be related to the maximum change of mean temperature distribution,

$$e = \frac{\overline{T}^{I+1} - \overline{T}^{I}}{\overline{T}^{I+1}}. \tag{8}$$

2.1 Evaluation of the mean temperature field

In this section we discuss a suitable procedure to evaluate the mean temperature $\overline{T}$ within the shell structure. The strong form of the corresponding static boundary value problem [2] reads in the absence of internally generated heat

$$\overline{kT}_{,ii} = 0 \ , \tag{9}$$

$$\overline{T} = T_0 \ \text{ at } \ \Gamma_T \ , \tag{10}$$

$$q_0 = q_n = -\overline{kT}_{,i} n_i \ \text{ at } \ \Gamma_q \ . \tag{11}$$

Equation (9) refers to the energy balance with $\overline{k}$ denoting the mean value of thermal conductivity. A comma within an index denotes a partial derivative and Einstein's sum convention is understood ($i = \hat{x}, \hat{y}$). The Dirichlet boundary condition is depicted in (10), where mean temperatures are prescribed to a given value T_0 at the boundary Γ_T. The corresponding von Neumann boundary condition at Γ_q with the normal direction n_i is given in (11), where the heat flux in normal direction q_n is prescribed to q_0. The mean value of thermal conductivity can be evaluated as usual, i.e.

$$\overline{k} = 1/h \int_h k(\hat{z})\, d\hat{z}. \tag{12}$$

However, a modified value of $\overline{k}$ can be given by considering thermal conduction as

$$q_i = -k(\hat{z})T_{,i}(\hat{x},\hat{y},\hat{z}). \tag{13}$$

By integration (13) with respect to the thickness direction we get

$$\int_h q_i d\hat{z} = -\int_h k(\hat{z})T_{,i}(\hat{x},\hat{y},\hat{z})d\hat{z} = -\int_h k(\hat{z})\overline{T}_{,i}(\hat{x},\hat{y})\theta_2(\hat{z})d\hat{z}, \tag{14}$$

where we have incorporated the decomposition (2) in connection with (5). Equation (14) leads to

$$\overline{T}_{,i}(\hat{x},\hat{y})\int_h k(\hat{z})\theta_2(\hat{z})d\hat{z} = \overline{T}_{,i}(\hat{x},\hat{y})\overline{k}h, \tag{15}$$

and the mean value of thermal conductivity reads

$$\overline{k} = {}^1\!/_h \int_h k(\hat{z})\theta_2(\hat{z})d\hat{z}. \tag{16}$$

The evaluation of the mean value of thermal conductivity according to (16) requires $\theta_2(\hat{z})$ which is found a posteriori based on $\overline{T}$ (see Algor. 1). The weak form of (9)-(11) is found from weighted residuals,

$$\int_V \overline{k}\,\overline{T}_{,ii}\delta\overline{T}dV - \int_{\Gamma_q}(q_0 - q_n)\delta\overline{T}d\Gamma = 0, \tag{17}$$

where the weighting function $\delta\overline{T}$ is a virtual temperature distribution that satisfies the Dirichlet boundary condition ($\delta\overline{T} = 0$ at Γ_T). Usual manipulations of (17) including the application of the Gaussian theorem lead to

$$\int_V \overline{kT}_{,i}\delta\overline{T}_{,i}dV = -\int_{\Gamma_q} q_0\delta\overline{T}d\Gamma. \tag{18}$$

With classical bilinear interpolations for the mean temperature field and the virtual mean temperature field

$$\overline{T}(\xi,\eta) = \mathbf{N}(\xi,\eta)\overline{\mathbf{T}}^e \;\text{ and }\; \delta\overline{T} = \mathbf{N}(\xi,\eta)\delta\overline{\mathbf{T}}^e\ , \tag{19}$$

where $\overline{\mathbf{T}}^e$ and $\delta\overline{\mathbf{T}}^e$ denote the nodal mean temperatures and virtual nodal mean temperatures. The elemental parent coordinates ξ and η are introduced in standard manner $-1 \le \xi \le 1$ and $-1 \le \eta \le 1$ and the relation to Cartesian coordinates is given with

$$\begin{bmatrix} \hat{x} \\ \hat{y} \end{bmatrix} = \begin{bmatrix} \mathbf{N} & \mathbf{0} \\ \mathbf{0} & \mathbf{N} \end{bmatrix} \begin{bmatrix} \hat{\mathbf{X}} \\ \hat{\mathbf{Y}} \end{bmatrix}, \tag{20}$$

where $\hat{\mathbf{X}}$ and $\hat{\mathbf{Y}}$ refer to the nodal coordinates. We get for the left hand side of (18) on element level

$$\int_V \overline{kT}_{,i}\delta\overline{T}_{,i}\,dV = \left(\delta\overline{\mathbf{T}}^e\right)^T \overline{k}h \int_{-1}^{1}\int_{-1}^{1} \mathbf{B}^T\mathbf{B}\det\mathbf{J}\,d\xi d\eta\overline{\mathbf{T}}^e = \left(\delta\overline{\mathbf{T}}^e\right)^T \mathbf{K}_T^e\overline{\mathbf{T}}^e\ , \tag{21}$$

with $\mathbf{B}$ referring to the spatial gradient of the shape functions, i.e.

$$\mathbf{B} = \begin{bmatrix} \mathbf{B}_{\hat{x}} \\ \mathbf{B}_{\hat{y}} \end{bmatrix} = \begin{bmatrix} N_{1,\hat{x}} & N_{2,\hat{x}} & N_{3,\hat{x}} & N_{4,\hat{x}} \\ N_{1,\hat{y}} & N_{2,\hat{y}} & N_{3,\hat{y}} & N_{4,\hat{y}} \end{bmatrix}. \tag{22}$$

The matrix $\mathbf{K}_T^e$ represents elemental thermal stiffness matrix. The term on the right hand side of (18) is devoted to convection on the top and bottom side of the shell which is modeled according to (6). We can write

$$\begin{aligned} -\int_{\Gamma_q} q_0\delta\overline{T}\,d\Gamma = &-\left(\delta\overline{\mathbf{T}}^e\right)^T \int_{-1}^{1}\int_{-1}^{1} (h_{ct}+h_{cb})\,\mathbf{N}^T\mathbf{N}\det\mathbf{J}\,d\xi d\eta\overline{T}^e + \\ &+\left(\delta\overline{\mathbf{T}}^e\right)^T \int_{-1}^{1}\int_{-1}^{1} (h_{ct}T_{Bt}^* + h_{cb}T_{Bb}^*)\,\mathbf{N}^T\det\mathbf{J}\,d\xi d\eta \\ &= -\left(\delta\overline{\mathbf{T}}^e\right)^T \mathbf{K}_{Tc}^e\overline{\mathbf{T}}^e + \left(\delta\overline{\mathbf{T}}^e\right)^T \mathbf{F}_{Tc}^e\ . \end{aligned} \tag{23}$$

The term $\det\mathbf{J}$ denotes the determinant of the elemental Jacobian $\mathbf{J}$,

$$\mathbf{J} = \begin{bmatrix} \partial\hat{x}/\partial\xi & \partial\hat{y}/\partial\xi \\ \partial\hat{x}/\partial\eta & \partial\hat{y}/\partial\eta \end{bmatrix}. \tag{24}$$

In connection with (18), (21) and (23) the algebraic system of equations on element level reads

$$\left(\mathbf{K}_T^e + \mathbf{K}_{Tc}^e\right)\overline{\mathbf{T}}^e = \mathbf{F}_{Tc}^e, \tag{25}$$

which has to be assembled to a global system in a standard manner [3]. All integrations over the elemental domain are carried out numerically using a 2×2 Gauss integration.

2.2 Evaluation of the transverse temperature field

Once the mean temperature $\overline{T}(\hat{x},\hat{y})$ is evaluated at every point of the shell's structure by the procedures discussed in Sect. 2.1, the temperature distribution with respect to the thickness direction is calculated next. Thereby, we analyze the problem depicted in Fig. 2a which shows an infinitesimal volume portion with cross section dA and height h, where a convection boundary condition on the top and bottom surface is applied. In

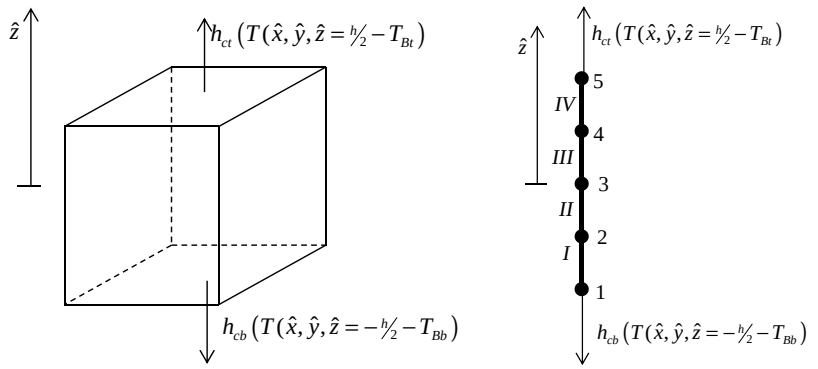

(a) Problem of transverse temperature distribution

(b) Discretized problem of transverse temperature distribution ($n = 4$)

Figure 2: Transverse temperature distribution

what follows we discuss a procedure where the temperature distribution with respect to the thickness direction is found based on a thermal conduction problem in connection with the two von Neumann boundary conditions. Thus, at every membrane location $\hat{x}$ and $\hat{y}$ (Fig. 1b) the following system of equations hold

$$\frac{d}{d\hat{z}}\left(k(\hat{x})\frac{d}{d\hat{z}}T(\hat{z})\right) + K^* = 0\ , \tag{26}$$

$$\hat{z} = h/2: \ -k(\hat{z}=h/2)\left.\frac{dT(\hat{z})}{d\hat{z}}\right|_{\hat{z}=h/2} - h_{ct}\,(T(\hat{z}=h/2) - T_{Bt}) = 0\ , \tag{27}$$

$$\hat{z} = -h/2: \ -k(\hat{z}=-h/2)\left.\frac{dT(\hat{z})}{d\hat{z}}\right|_{\hat{z}=-h/2} - h_{ct}\,(T(\hat{z}=-h/2) - T_{Bb}) = 0\ . \tag{28}$$

There, a crucial step is the introduction of K^* which is related to the variation of thermal conductivity, i.e.

$$K^* = Kk(\hat{z}), \tag{29}$$

where K represents an unknown constant. The inclusion of (29) in (26) is mandatory for accurate results and is in contrast to [4] where a similar strong form is used without K^*. The inclusion of the constant K^* can be motivated by the following thought experiment: Consider a shell's portion with a constant thermal conductivity then the transverse temperature distribution is expected to be parabolical with prescribed gradients at the top and bottom surface. However, in the absence of K^* the solution of (26) leads only to a linear distribution and (27) and (28) cannot be satisfied properly. Only a non-vanishing constant K^* can lead to correct results. The unknown constant K is found by demanding that the mean value of $T(\hat{x},\hat{y},\hat{z})$ equals the evaluated mean value found with the procedures discussed in Sect. 2.1 (see (1)). Suitable solution procedures

of equations (26) - (28) require the decomposition introduced in (2). Rewriting (26)-(28) with $T(\hat{x},\hat{y},\hat{z}) = \overline{T}(\hat{x},\hat{y}) + \theta_1(\hat{z})$ leads to

$$\frac{d}{d\hat{z}}\left(k(\hat{z})\frac{d}{d\hat{z}}\theta_1(\hat{z})\right) + Kk(\hat{z}) = 0\ , \tag{30}$$

$$\hat{z} = {}^{h}/_{2}:\ -k(\hat{z}={}^{h}/_{2})\left.\frac{d\theta_1(\hat{z})}{d\hat{z}}\right|_{\hat{z}={}^{h}/_{2}} - h_{ct}\left(\overline{T} + \theta_1(\hat{z}=-{}^{h}/_{2}) - T_{Bt}\right) = 0\ , \tag{31}$$

$$\hat{z} = -{}^{h}/_{2}:\ -k(\hat{z}=-{}^{h}/_{2})\left.\frac{d\theta_1(\hat{z})}{d\hat{z}}\right|_{\hat{z}=-{}^{h}/_{2}} - h_{ct}\left(\overline{T} + \theta_1(\hat{z}=-{}^{h}/_{2}) - T_{Bb}\right) = 0\ , \tag{32}$$

$$\int_h \theta_1(\hat{z})\,d\hat{z} = 0\ . \tag{33}$$

We propose a FEM like solution procedure for (30)-(33). There, a discretization of Fig. 2a with respect to $\hat{z}$ with n linear elements of length $l_e = {}^{h}/_{n}$ is necessary (see Fig. 2b). We may write for the interior elements (elements II and III in Fig. 2b)

$$dA\int_{l_e} k(\hat{z})\theta_{,\hat{z}}\delta\vartheta_{,\hat{z}}\,d\hat{z} = dAK\int_{l_e} k(\hat{z})\delta\theta\,d\hat{z} \tag{34}$$

leading to a linear algebraic system of equations on element level of

$$\frac{k_m}{l_e}\begin{bmatrix} 1 & -1 \\ -1 & 1 \end{bmatrix}\begin{bmatrix} \vartheta_1^e \\ \vartheta_2^e \end{bmatrix} = \frac{l_e K k_m}{2}\begin{bmatrix} 1 \\ 1 \end{bmatrix}. \tag{35}$$

In (34) we use for $k(\hat{z})$ the value of thermal conductivity at the element's center in the middle between the two nodes 1 and 2 which is denoted by k_m. The unknown nodal constants are denoted with ϑ_1^e and ϑ_2^e. For the bottom and top element (elements I and IV in Fig. 2b) the von Neumann boundary condition (32) and (31) has to be included. In connection to (17) we get for the undermost element

$$dA\int_{l_e} k(\hat{z})\theta_{1,\hat{z}}\delta\theta_{1,\hat{z}}\,d\hat{z} = dA\int_{l_e} K^*\delta\theta_1\,d\hat{z} - \left(h_{cb}dA\left(\overline{T} + \theta_1 - T_{Bb}\right)\delta\theta_1\right)\big|_{\hat{z}=-h/2}\,, \tag{36}$$

leading to

$$\left\{\frac{k_m}{l_e}\begin{bmatrix} 1 & -1 \\ -1 & 1 \end{bmatrix} + \begin{bmatrix} h_{cb} & 0 \\ 0 & 0 \end{bmatrix}\right\}\begin{bmatrix} \vartheta_1^e \\ \vartheta_2^e \end{bmatrix} = \frac{l_e K k_m}{2}\begin{bmatrix} 1 \\ 1 \end{bmatrix} + \begin{bmatrix} h_{cb}\left(T_{Bb} - \overline{T}\right) \\ 0 \end{bmatrix}, \tag{37}$$

and for the uppermost

$$dA\int_{l_e} k(\hat{z})\theta_{1,\hat{z}}\delta\theta_{1,\hat{z}}\,d\hat{z} = dA\int_{l_e} K^*\delta\theta_1\,d\hat{z} - \left(h_{ct}dA\left(\overline{T} + \theta_1 - T_{Bt}\right)\delta\theta_1\right)\big|_{\hat{z}=h/2}\,, \tag{38}$$

and further

$$\left\{ \frac{k_m}{l_e} \begin{bmatrix} 1 & -1 \\ -1 & 1 \end{bmatrix} + \begin{bmatrix} 0 & 0 \\ 0 & h_{ct} \end{bmatrix} \right\} \begin{bmatrix} \vartheta_1^e \\ \vartheta_2^e \end{bmatrix} = \frac{l_e K k_m}{2} \begin{bmatrix} 1 \\ 1 \end{bmatrix} + \begin{bmatrix} 0 \\ h_{ct} \left(T_{Bt} - \overline{T} \right) \end{bmatrix}. \tag{39}$$

A suitable assembly of the system of equations on element level ((35), (37) and (39)) gives for the discretization of Fig. 2b with four elements ($n = 4$)

$$\left\{ \frac{4}{h} \begin{bmatrix} k_1 & -k_1 & 0 & 0 & 0 \\ -k_1 & k_1 + k_2 & -k_2 & 0 & 0 \\ 0 & -k_2 & k_2 + k_3 & -k_3 & 0 \\ 0 & 0 & -k_3 & k_3 + k_4 & -k_4 \\ 0 & 0 & 0 & -k_4 & k_4 \end{bmatrix} + \begin{bmatrix} h_{cb} & 0 & 0 & 0 & 0 \\ 0 & 0 & 0 & 0 & 0 \\ 0 & 0 & 0 & 0 & 0 \\ 0 & 0 & 0 & 0 & 0 \\ 0 & 0 & 0 & 0 & h_{ct} \end{bmatrix} \right\} \begin{bmatrix} \vartheta_1 \\ \vartheta_2 \\ \vartheta_3 \\ \vartheta_4 \\ \vartheta_5 \end{bmatrix} =$$

$$= K \frac{h}{8} \begin{bmatrix} k_1 \\ k_1 + k_2 \\ k_2 + k_3 \\ k_3 + k_4 \\ k_4 \end{bmatrix} + \begin{bmatrix} h_{cb} \left(T_{Bb} - \bar{T} \right) \\ 0 \\ 0 \\ 0 \\ h_{ct} \left(T_{Bt} - \bar{T} \right) \end{bmatrix}, \tag{40}$$

where the thermal conductivities k_i for $i = 1, 2, 3, 4$ represent the conductivity at the i-th element center. Equation (40) can be rewritten according to

$$\mathbf{K}\boldsymbol{\vartheta} = K\mathbf{F} + \mathbf{F}_c, \tag{41}$$

and represents a linear algebraic system of equations approximating (30) - (32). The demand of a vanishing mean value of ϑ (33) is modeled as

$$\begin{bmatrix} 1/2 & 1 & 1 & 1 & 1/2 \end{bmatrix} \begin{bmatrix} \vartheta_1 \\ \vartheta_2 \\ \vartheta_3 \\ \vartheta_4 \\ \vartheta_5 \end{bmatrix} = \mathbf{L}\boldsymbol{\vartheta} = 0. \tag{42}$$

Equation (42) is used to evaluate the unknown constant K leading to

$$K = -\frac{\mathbf{L}\mathbf{K}^{-1}\mathbf{F}_c}{\mathbf{L}\mathbf{K}^{-1}\mathbf{F}}, \tag{43}$$

and, consequently, the nodal constants $\boldsymbol{\vartheta}$ read

$$\boldsymbol{\vartheta} = -\frac{\mathbf{L}\mathbf{K}^{-1}\mathbf{F}_c}{\mathbf{L}\mathbf{K}^{-1}\mathbf{F}} \mathbf{K}^{-1}\mathbf{F} + \mathbf{K}^{-1}\mathbf{F}_c. \tag{44}$$

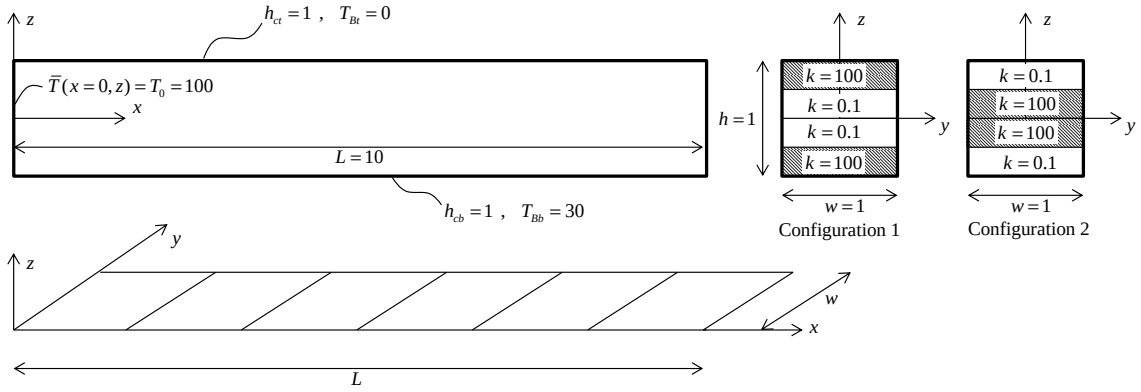

Figure 3: FGM fin with a discretization of $N = 6$

3 Numerical example

For sake of space, only one benchmark problem is introduced here which shows the importance of temperature variations with respect to the thickness direction and the good predictive quality of the correspondingly proposed algorithm. Consider a rectangular MLC structure of length $L = 10$, width $w = 1$ and height $h = 1$ shown in Fig. 3 which is discretized with N elements. On the top and bottom surface ($z = \pm h/2$) a convection boundary condition with a convection coefficient of $h_{ct} = 1$ and $h_{cb} = 1$, and a fluid temperature of $T_{Bt} = 0$ and $T_{Bb} = 30$ is applied, while the left end at $x = 0$ shows a Dirichlet boundary condition with $\overline{T}(x = 0) = T_0 = 100$. The fin is composed by four equidistant layers of height $h_L = h/4$, each with a different thermal conductivity. We compare two symmetric configurations (i.e. Configuration 1 and Configuration 2) according to Fig. 3). Configuration 1 is characterized by a high thermal conductivity on the top and bottom layer while configuration 2 has nearly isolating outside layers. We observe that the mean value of thermal conductivity, i.e. $\overline{k} = 1/h \int_h k(z)dz$, is equal for both configurations and many authors expect the same temperature distribution in membrane direction. The reference results are evaluated using ANSYS by discretizing the $x - z$ plane with 500×100 PLANE55 elements [5]. The application of a Dirichlet boundary condition, i.e. $T(x = 0, z) = T_0$, is in contrast to the applied convection boundary conditions at $x = 0$, $z = \pm h/2$, since the thermal gradient with respect to the thickness direction is not vanishing on the top and bottom side. Therefore, we apply a von Neumann boundary condition onto the ANSYS model based on the Fourier's law of thermal conduction, i.e.

$$q_n(x = 0,\ z) = -k(z)\overline{T}_{,x} = Ck(z), \tag{45}$$

where the constant C is found iteratively so that the evaluated mean value of the temperature distribution at $x = 0$ equals T_0. Accordingly we get for the two configurations

$$q_n^{Config1}(x = 0,\ z) = -16.3613k(z), \tag{46}$$

$$q_n^{Config2}(x = 0,\, z) = -8.7069k(z). \tag{47}$$

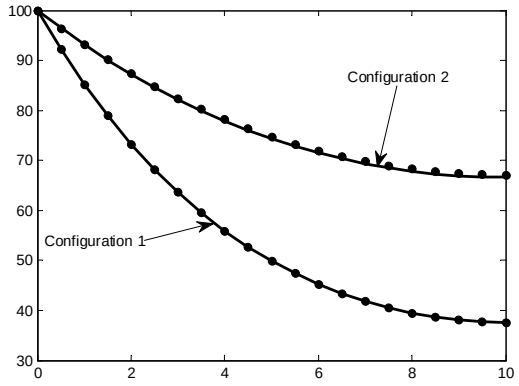

Figure 4: Mean temperature distribution of both configurations $N = 20$, $n = 40$

The distribution of the mean value of temperature is depicted in Fig. 4, where we used $N = 20$ shell elements in membrane direction and 10 elements through each layer in transverse direction ($n = 40$). There, the solid line corresponds to the present approach, while the dots refer to the ANSYS solution. Fig. 4 indicates good accuracy of the proposed solution algorithm for both configurations, and we observe large differences between the two configurations, even if the average value of the thermal conductivity is identical.

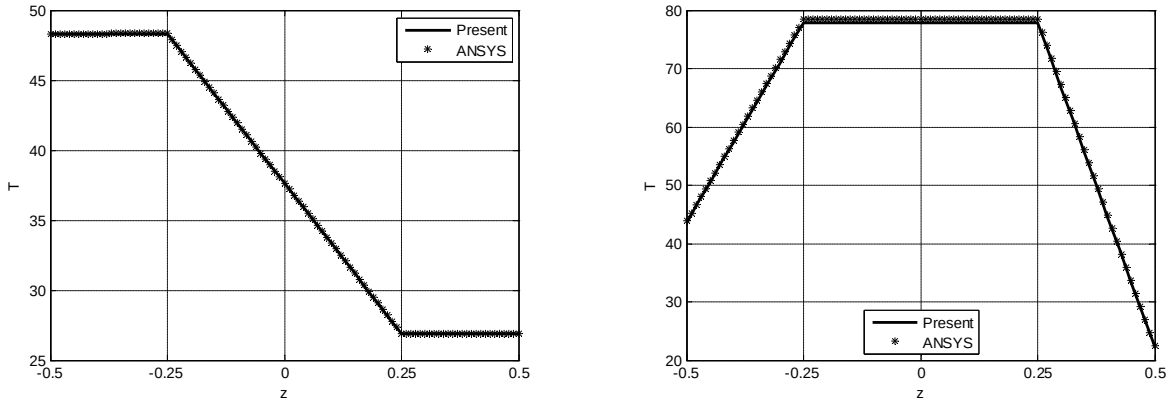

(a) Configuration 1 (b) Configuration 2

Figure 5: Temperature distribution in transverse direction at $x = L$, ($N = 20$, $n = 40$)

Furthermore, the temperature distribution in transverse direction also depends quantitatively and qualitatively on the configuration in use (see Fig. 5 which, again, indicates

a good predictive quality of the proposed approach).

4 Conclusion

In this paper an iterative algorithm is presented which evaluates temperature distributions in shell structures made of functionally graded materials. Convection boundary conditions are applied on the top and bottom surface. The crucial step is the decomposition of the temperature distribution into a membrane and a transverse field, respectively. Both fields are evaluated consecutively and the accuracy of the proposed formulations is shown in one benchmark example.

Acknowledgment:

This paper has been supported by Grant Agency VEGA - Project Number: 1/0534/12, and by APVV-0246-12.

REFERENCES

[1] B. Abbasnejad, G. Rezazadeh, Mechanical behavior of a fgm micro-beam subjected to a nonlinear electrostatic pressure, *International Journal of Materials and Design* 8 (2012) 381–392.

[2] A. Mills, Basic Heat and Mass Transfer, *Prentice Hall*, 1999.

[3] O. C. Zienkiewicz, R. L. Taylor, Finite Element Method: Volume 1, The Basis (Finite Element Method), *Butterworth-Heinemann*, 2000.

[4] R. Naghdabadi, S. H. Kordkheili, A finite element formulation for analysis of functionally graded plates and shells, *Archive of applied mechanics* 74 (2005) 375–386.

[5] ANSYS, Ansys V11 Documentation.